# *Mycobacterium tuberculosis* carrying a rifampicin drug resistance mutation reprograms macrophage metabolism through cell wall lipid changes

Nicole C. Howard[1], Nancy D. Marin[1], Mushtaq Ahmed[1], Bruce A. Rosa[2], John Martin[2], Monika Bambouskova[3], Alexey Sergushichev[4], Ekaterina Loginicheva[3], Natalia Kurepina[5], Javier Rangel-Moreno[6], Liang Chen[5], Barry N. Kreiswirth[5], Robyn S. Klein[2], Joan-Miquel Balada-Llasat[7], Jordi B. Torrelles[8,9], Gaya K. Amarasinghe[3], Makedonka Mitreva[2], Maxim N. Artyomov[3], Fong-Fu Hsu[2], Barun Mathema[10], and Shabaana A. Khader[1]

*[1]Department of Molecular Microbiology, [2]Department of Medicine, [3]Department of Pathology and Immunology, Washington University School of Medicine, St. Louis, MO, 63110; [4]Computer Technologies Department, ITMO University, Saint Petersburg, Russia, 197101; [5]Public Health Research Institute, New Jersey Medical School, Rutgers University, Newark, NJ, 07103; [6]Division of Allergy/Immunology and Rheumatology, University of Rochester School of Medicine and Dentistry, Rochester, NY, 14642; [7]Department of Pathology, [8]Department of Microbial Infection and Immunity, The Ohio State University, Columbus, OH, 43210; [9]Texas Biomedical Research Institute, San Antonia, TX, 78227; [10]Department of Epidemiology, Columbia University Mailman School of Public Health, New York, NY, 10032*

*__Corresponding Author__- Shabaana A. Khader, Department of Molecular Microbiology, Campus Box 8230, 660 South Euclid Avenue, St. Louis, MO, 63110-1093, Phone: (314) 286-1590, Fax: (314) 362-1232, Email: sakhader@wustl.edu

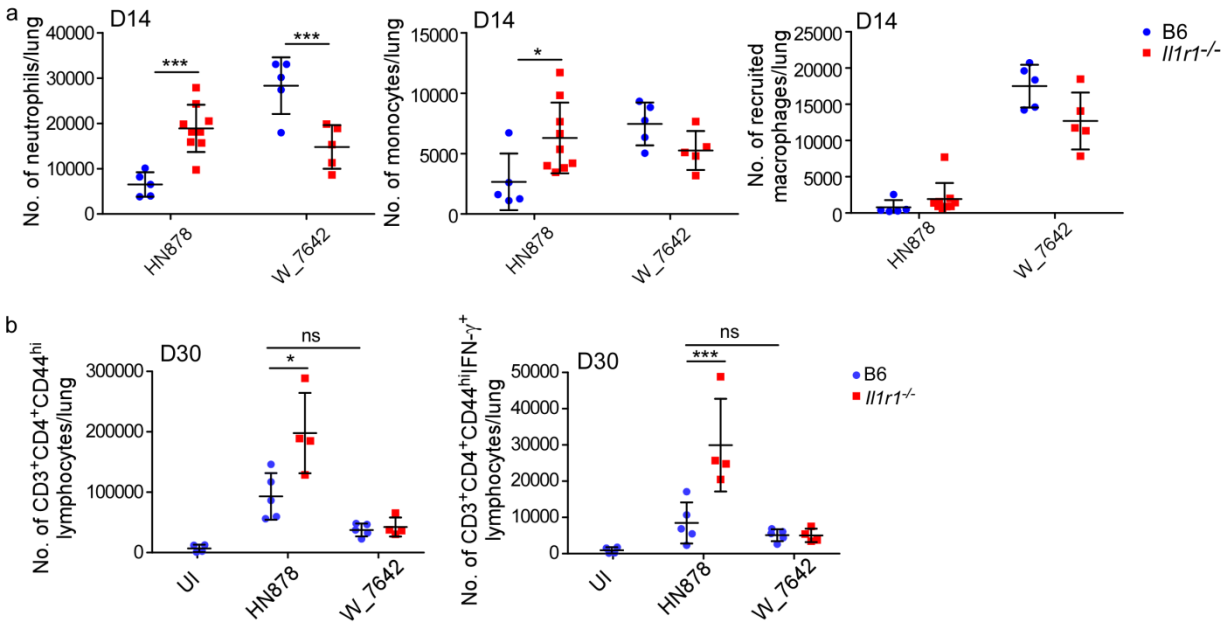


Howard et al., Supplementary Figure 1

**Supplementary Figure 1. B6 and *Il1r1*$^{-/-}$ mice generate similar immune responses upon infection with W_7642.** B6 and *Il1r1*$^{-/-}$ mice were aerosol infected with 100 CFU *Mtb* HN878 or W_7642 (B6 n=5, *Il1r1*$^{-/-}$ n=9 (HN878), n=5 (W_7642)). Lungs were processed to a single cell suspension, and the total numbers of neutrophils, monocytes and recruited macrophages were determined 14 dpi (a). B6 and *Il1r1*$^{-/-}$ mice were aerosol infected with 100 CFU *Mtb* HN878 or W_7642 (B6 n=5, *Il1r1*$^{-/-}$ n=4, UI n=4). Lungs were processed to a single cell suspension, and the total numbers of $CD3^{+}CD4^{+}CD44^{hi}$ cells and $CD3^{+}CD4^{+}CD44^{hi}$IFN-$\gamma^{+}$ cells were determined by flow cytometry on 30 dpi (b). UI-uninfected. (a,b) 1-way ANOVA with Tukey's post-test. The data points represent the mean (±SD) of values. *p≤0.05, ***p≤0.001, ns-not significant (p>0.05).

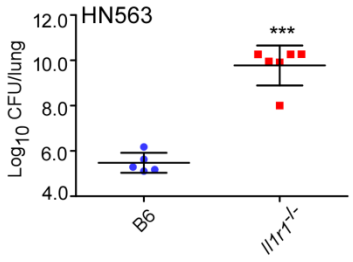


Howard et al., Supplementary Figure 2

**Supplementary Figure 2. IL-1R1 is required for protection against *Mtb* HN563.** B6 and *Il1r1*$^{-/-}$ mice were aerosol infected with 100 CFU W-Beijing *Mtb* HN563, and lung bacterial burden was determined by plating on 30 dpi (B6 n=5, *Il1r1*$^{-/-}$ n=6). Two tailed Student's t-test. The data points represent the mean (±SD) of values. ***p≤0.001.

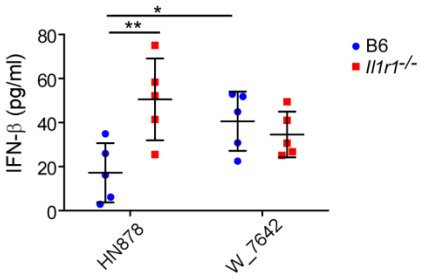


Howard et al., Supplementary Figure 3

**Supplementary Figure 3. W_7642 *in vivo* infection induces increased lung IFN-β levels.** B6 and *Il1r1*$^{-/-}$ mice were aerosol infected with 100 CFU *Mtb* HN878 or W_7642. On 30 dpi, IFN-β protein levels were measured in lung homogenates (n=5). 1-way ANOVA with Tukey's post-test. The data points represent the mean (±SD) of values. *p≤0.05, **p≤0.01.

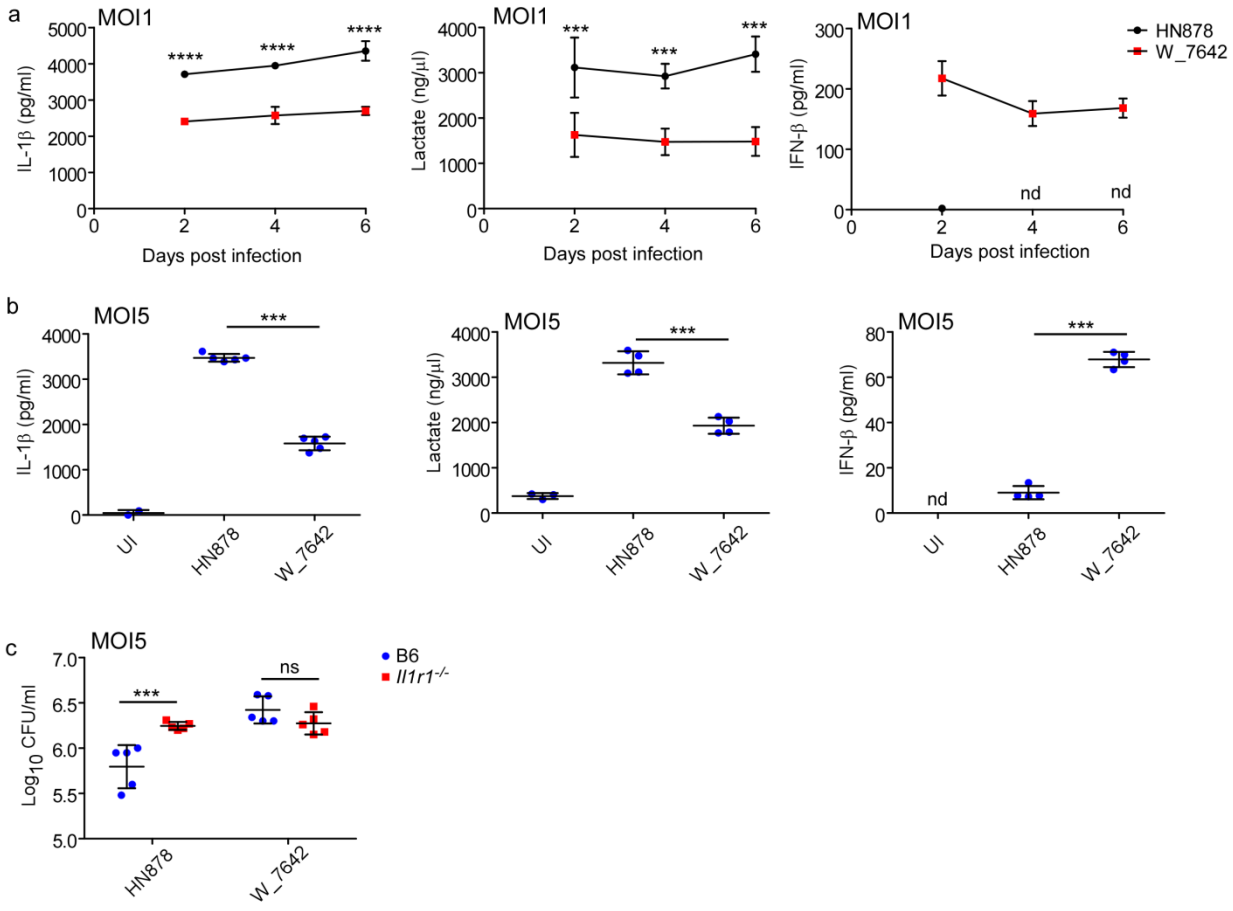


Howard et al Supplementary Figure 4

**Supplementary Figure 4. HN878 and W_7642 induce different immune responses during macrophage infection at varying time points and MOIs.** B6 and *Il1r1*$^{-/-}$ macrophages were infected with HN878 or W_7642 (MOI1, n=4) and IL-1β, lactate and IFN-β protein levels were determined at 2, 4, and 6 dpi (a). B6 and *Il1r1*$^{-/-}$ macrophages were infected with HN878 or W_7642 (MOI5) and IL-1β (n=5), lactate and IFN-β (n=4) protein levels (b) and intracellular CFU (c, n=5) were determined at 6 dpi. UN-untreated, nd-not detectable. (a) 2-way ANOVA with Bonferroni post-test, (b,c) 1-way ANOVA with Tukey's post-test. The data points represent the mean (±SD) of values. ***p≤0.001, ****p≤0.0001, ns-not significant (p>0.05).

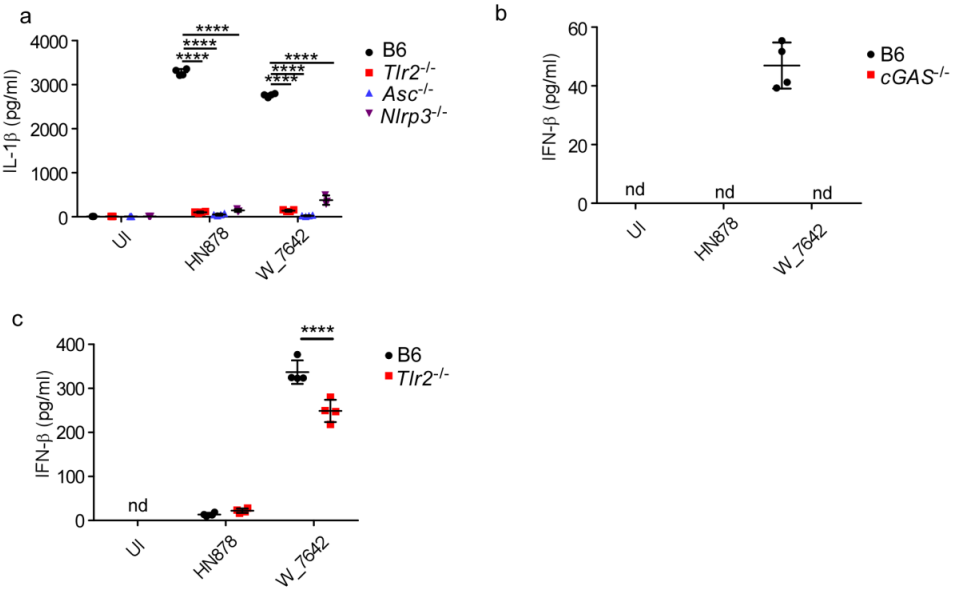


Howard et al., Supplementary Figure 5

**Supplementary Figure 5. *Mtb* induced IL-1β is TLR2-dependent, while IFN-β induction is cGAS-dependent.** IL-1β levels were measured in the supernatants of DCs from B6, *Tlr2*$^{-/-}$, *Asc*$^{-/-}$, and *Nlrp3*$^{-/-}$ mice 2 dpi upon HN878 or W_7642 infection (MOI1, n=4) (a). IFN-β levels were measured in the supernatants of macrophages from B6 and *cGAS*$^{-/-}$ mice on 2 dpi following HN878 or W_7642 infection (MOI1, n=4) (b). IFN-β levels were measured in the supernatants of DCs from B6 and *Tlr2*$^{-/-}$ mice at 2 dpi upon infection with HN878 or W_7642 (MOI1, n=4) (c). UI-uninfected, nd-not detectable. (a-c) 2-way ANOVA with Bonferroni post-test. The data points represent the mean (±SD) of values. ****p≤0.0001.

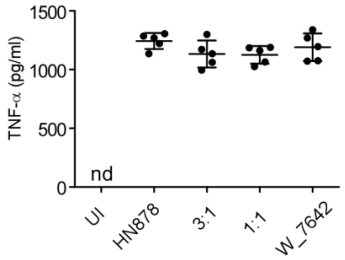


Howard et al., Supplementary Figure 6

**Supplementary Figure 6. Co-infection of B6 macrophages with HN878 and W_7642 does not alter TNF-α production**. B6 macrophages were infected with HN878 and W_7642 alone or in combination (3 HN878:1 W_7642, 1 HN878:1 W_7642, total MOI1, n=5 per condition). TNF-α protein was measured in supernatants. UI-uninfected, nd-not detectable. 1-way ANOVA with Tukey's post-test. The data points represent the mean (±SD) of values.

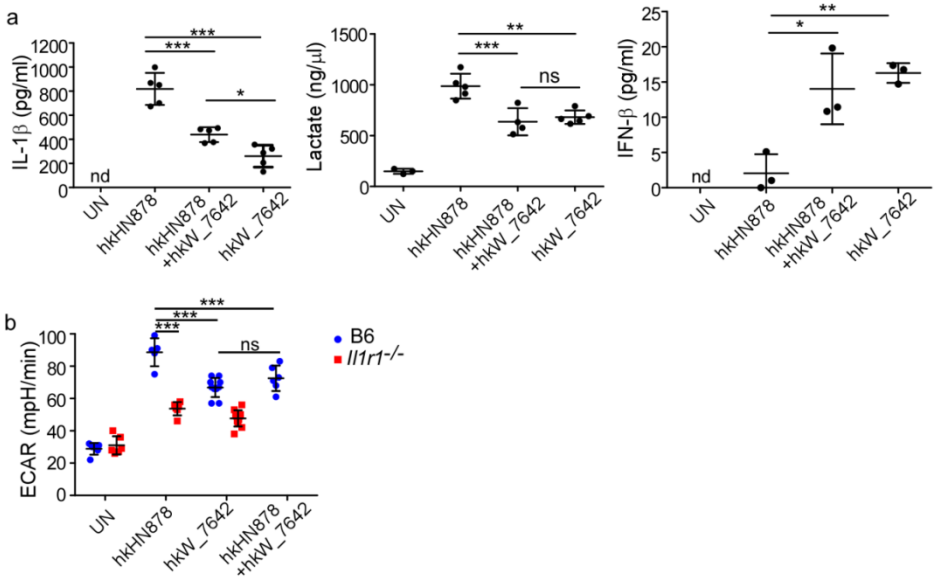


Howard et al Supplementary Figure 7

**Supplementary Figure 7. Hk *Mtb* mimics metabolic rewiring in macrophages induced by live *Mtb* infection.** B6 and *Il1r1*$^{-/-}$ macrophages were treated with hkHN878, hkW_7642, or co-treated with both hkHN878 and hkW_7642 (20 µg/ml each) for 48 hours. Levels of IL-1β (n=5), lactate (n=4) and IFN-β (n=3) (a) were determined in supernatants, and ECAR (hkHN878 B6 n=5; UN, hkHN878 *Il1r1*$^{-/-}$, hkHN878 + hkW_7642 B6 n=6, hkW_7642 B6 n=10; hkW_7642 *Il1r1*$^{-/-}$ n=11) was measured in treated cells (b). UN-untreated, nd-not detectable. (a,b) 1-way ANOVA with Tukey's post-test. The data points represent the mean (±SD) of values. *p≤0.05, **p≤0.01, ***p≤0.001, ns-not significant (p>0.05).

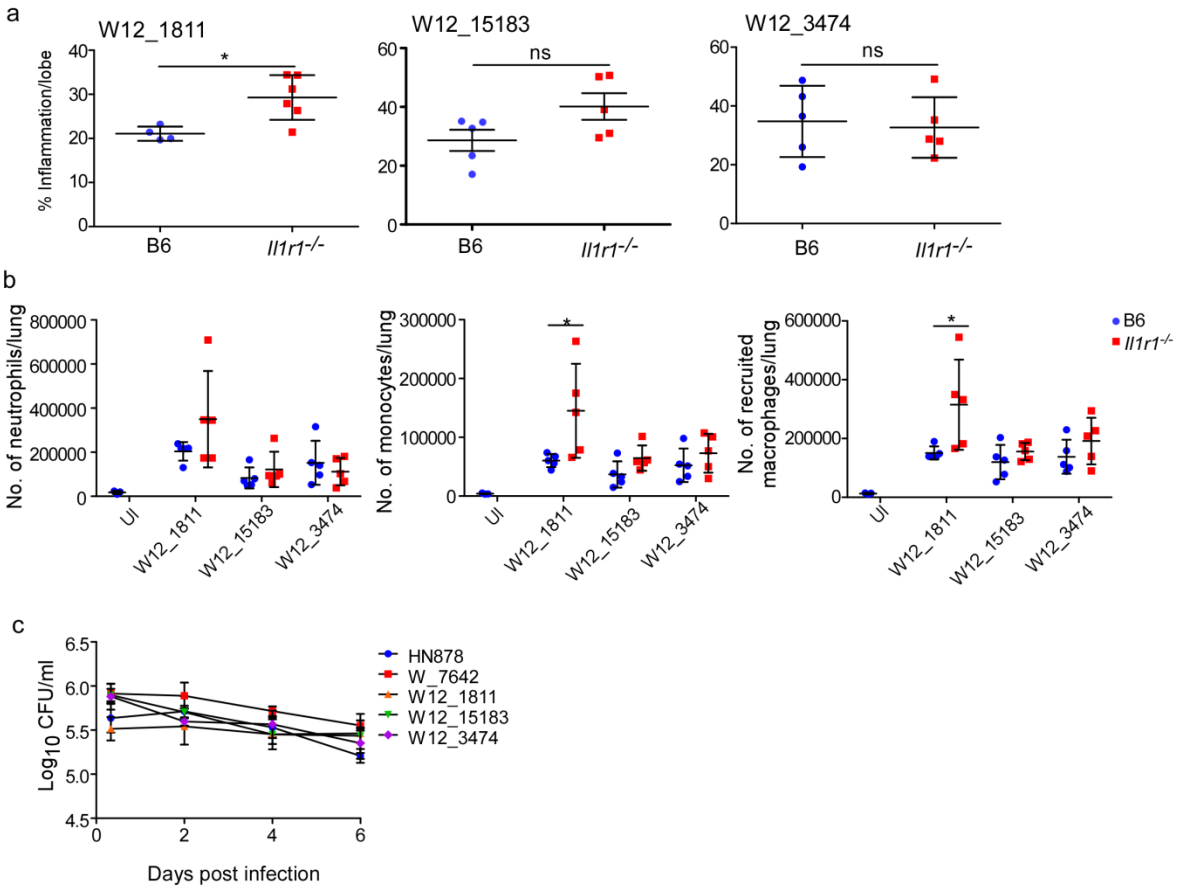


Howard et al., Supplementary Figure 8

**Supplementary Figure 8. Infection with W12_15183 or W12_3474 in *Il1r1*$^{-/-}$ mice does not exacerbate TB disease.** B6 and *Il1r1*$^{-/-}$ mice were aerosol infected with 100 CFU of the different *Mtb* strains. On 30 dpi, pulmonary histology was assessed by H&E staining on FFPE lung sections and inflammatory area was measured (a). The total number of neutrophils, monocytes, and recruited macrophages in the lung were assessed on 30 dpi (b, n=5, UI n=4). B6 macrophages were infected with different MDR *Mtb* strains (MOI1, n=4) and intracellular CFU was determined at different dpi (c). UI-uninfected. (a) Two tailed Student's t-test, (b,c) 2-way ANOVA with Bonferroni post-test. The data points represent the mean (±SD) of values. *p≤0.05, ns-not significant (p>0.05).

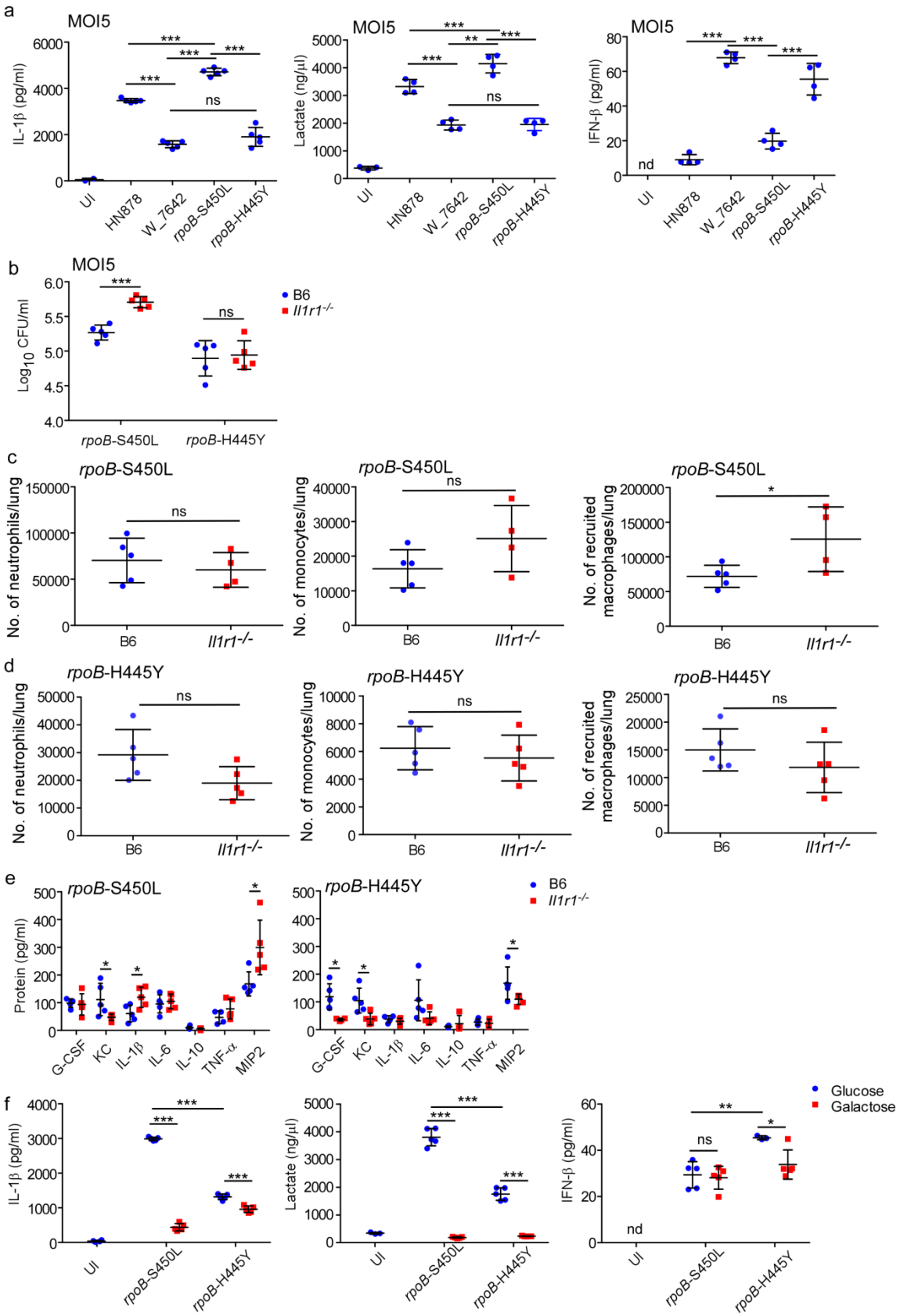


Howard et al Supplementary Figure 9

**Supplementary Figure 9. IL-1R1 signaling pathway is dispensable for protection with HN878 *rpoB*-H445Y mutant infection.** B6 and *Il1r1*$^{-/-}$ macrophages were infected with HN878, W_7642, HN878 *rpoB*-S450L or HN878 *rpoB*-H445Y (MOI5) and IL-1β (n=5), lactate and IFN-β (n=4) protein levels (a) and intracellular CFU (b, n=5) were determined at 6 dpi (HN878 and W_7642 datapoints are the same as shown in Supplementary Fig. 4b,c). B6 and *Il1r1*$^{-/-}$ mice were aerosol infected with HN878 *rpoB*-S450L or HN878 *rpoB*-H445Y at 100 CFU (HN878 *rpoB*-S450L B6, n=5; *Il1r1*$^{-/-}$, n=4; HN878 *rpoB*-H445Y n=5). On 30 dpi, the total number of neutrophils, monocytes, and recruited macrophages in the lung were assessed in lung single cell suspensions using flow cytometry (c,d). Cytokine and chemokine protein levels in lung homogenates were measured in B6 and *Il1r1*$^{-/-}$ mice at 30 dpi (e, n=5). B6 macrophages were infected with HN878 *rpoB*-S450L or *rpoB*-H445Y while in glucose or galactose (25mM each)-containing media. IL-1β (n=5), lactate (n=5), and IFN-β levels (n=5, except B6 *rpoB*-H445y, n=3) were determined 3 dpi (f). UN-untreated, nd-not detectable. (a,f) 1-way ANOVA with Tukey's post-test, (b,e) 2-way ANOVA with Bonferroni post-test, (c,d) two tailed Student's t-test. The data points represent the mean (±SD) of values. *p≤0.05, **p≤0.01, ***p≤0.001, ns-not significant (p>0.05).

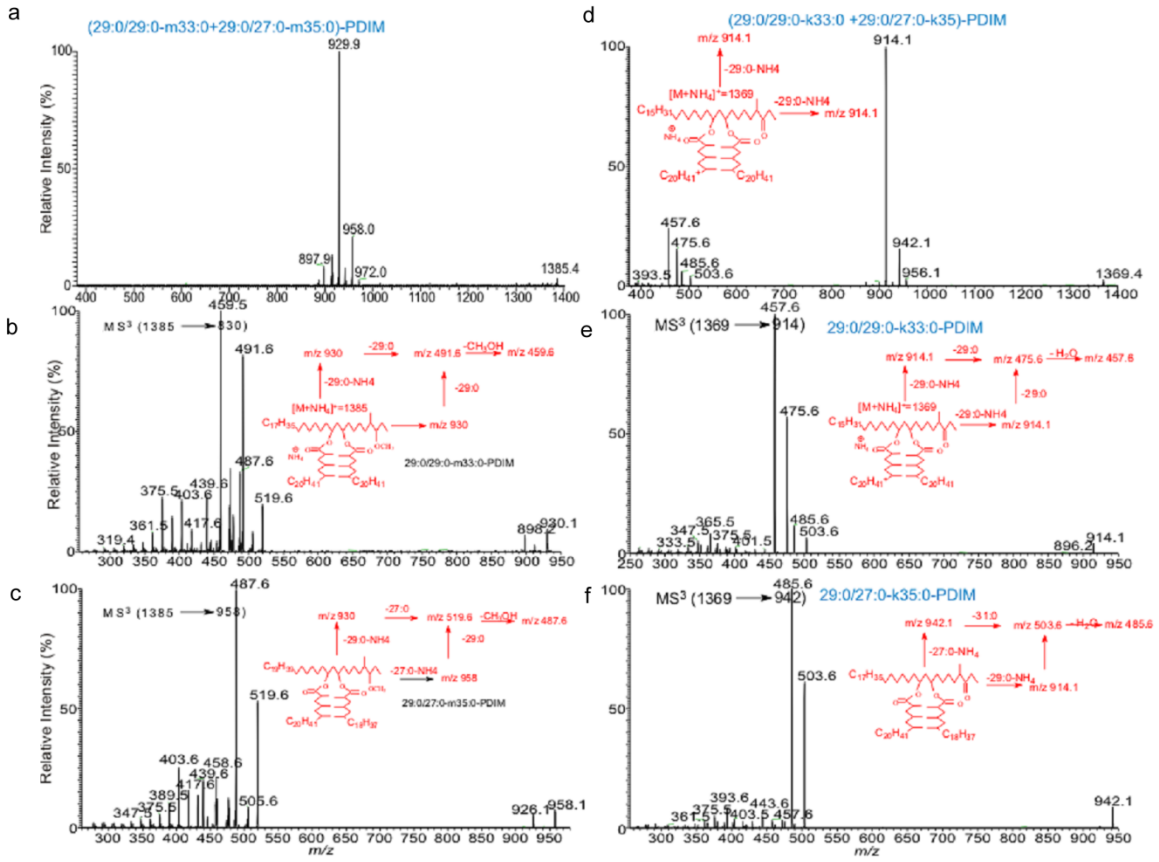


Howard et al., Supplementary Figure 10

**Supplementary Figure 10. Structural characterization of PDIMs by linear ion-trap multiple-stage tandem mass spectrometry.** Lipid extract from W_7642 was infused into a Thermo Obitrap Velos mass spectrometer. One in each methoxy (ion at m/z 1385) and keto (ion at m/z 1369) PDIM family was selected for structural characterization. High resolution mass measurement of the two ions gave 1385.4335 (calculated m/z: 1385.4326) and 1369.4018 (calculated m/z: 1369.4013), respectively, corresponding to the molecular formula of C92 H186 O5 N and C91 H182 O5 N, respectively.

$MS^2$ on the ion of m/z 1385 (a) gave rise to major ions at m/z 930 and 958, arising from cleavage of 29:0- and 27:0-fatty acid substituents as $NH_4^+$ salt, respectively. Further dissociation of the ion of m/z 930 (b; 1385 →930) gave rise to major ions at m/z 519 and 491, from further losses of 27:0- and 29:0-fatty acid substituents, respectively. The spectrum also contains ions of m/z 487, and 459, arising from loss of $CH_3OH$, consistent with the notion that the molecule belongs to the methoxy-PDIM family. The results indicate that the ions consist of 29:0/29:0-m33:0 and 29:0/27:0-m35:0-PDIM structures (see inset for the fragmentation scheme). The structural assignment is further confirmed by the $MS^3$ spectrum of the ion of m/z 958 (c; 1385 →958). The spectrum contains ions at m/z 519 from further loss of 27:0-FA residue, along with ion of m/z 487 arising from further loss of the methoxy side chain as $CH_3OH$. The results further support the assignment of the 29:0/27:0-m35:0 PDIM structure. Similar multiple-stage tandem mass spectrometric approaches were used to identify the structure of the ion of m/z 1369 (d-f). The $MS^2$ spectrum is dominated by the ion of m/z 914, arising from loss of 29:0-fatty acid as $NH_4^+$ salt, along with ion of m/z 942 arising from the corresponding 27:0-FA loss. Further dissociation of the ion of m/z 914 (e; 1369 →914) gave rise to ions of m/z 503 and 475 arising from losses of 27:0- and 29:0-fatty acid substituents respectively, along with ions of m/z 485 and 457, from further loss of $H_2O$ (see insets for the fragmentation scheme). The water loss is an indication that the compound belongs to the keto-PDIM family. The results led to the assignment

of the major 29:0/29:0-k33:0-PDIM structure, together with a 29:0/27:0-k35:0-PDIM isomer. The assignment is also further confirmed by the $MS^3$ spectrum of the ion of m/z 942 (f; 1369 →942), which gave major ions of m/z 503 (loss of 29:0-FA) and 485 (503 – $H_2O$), further supports the presence of the 29:0/27:0-k35:0-PDIM isomeric structure. One representative run is shown.

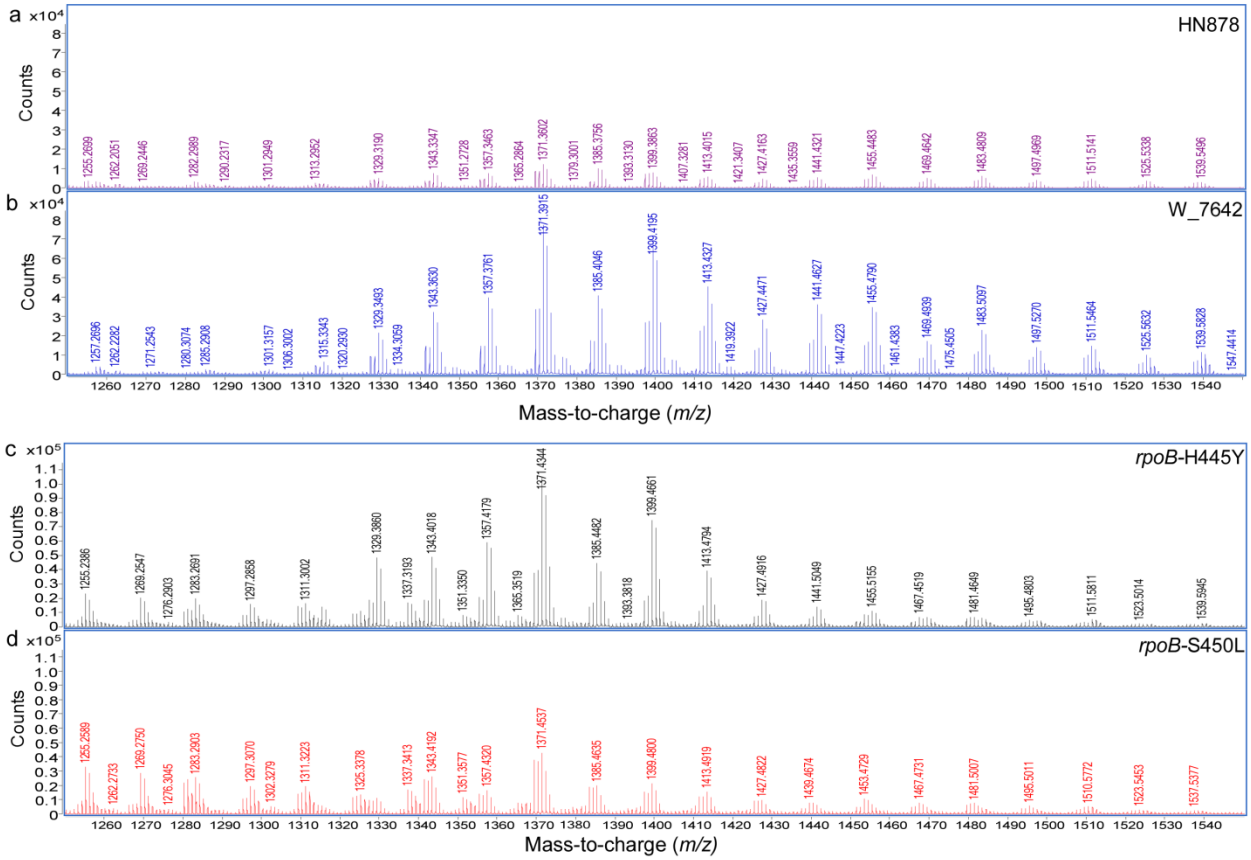


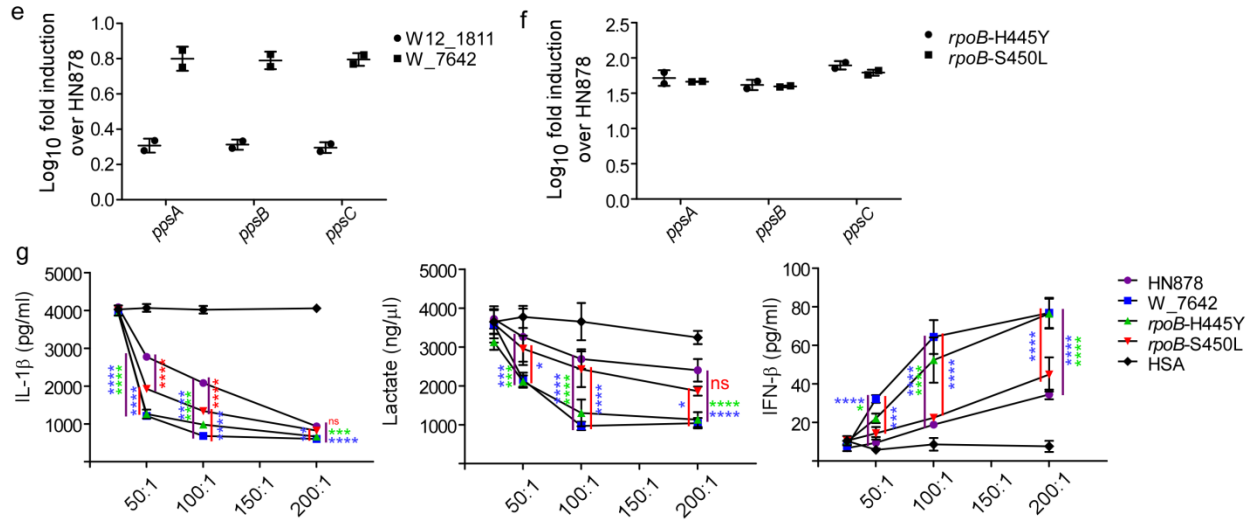





Howard et al., Supplementary Figure 11

**Supplementary Figure 11. PDIM overexpression in *rpoB* mutants.** PDIM spectra were generated from extracted total lipid from *Mtb* strains and relative abundance to the exogenously added internal standard TAG was determined for HN878 (a), W_7642 (b), *rpoB*-H445Y (c) and *rpoB*-S450L (d). Trace data is representative of at least two replicates. *ppsA*, *ppsB*, and *ppsC* mRNA expression was measured in W12_1811, W_7642 (e), and HN878 *rpoB*-H445Y and HN878 *rpoB*-S450L (f) and fold induction of mRNA over levels expressed in HN878 (n=2 per *Mtb* strain). PDIM was isolated from each *Mtb* strain and coated onto polystyrene beads. B6 macrophages (n=4 per treatment) were treated with PDIM coated beads (25:1, 50:1, 100:1 and 200:1) or HSA coated beads in combination with HN878 infection (MOI1). IL-1β, lactate and IFN-β protein levels were determined in 6 dpi supernatants (g). Comparisons between groups are colorized; the star and line color indicate which two groups are significantly different from each other. (g) 2-way ANOVA with Bonferroni post-test. The data points represent the mean (±SD) of values. *p≤0.05, **p≤0.01, ***p≤0.001, ****p≤0.0001, ns-not significant (p>0.05).

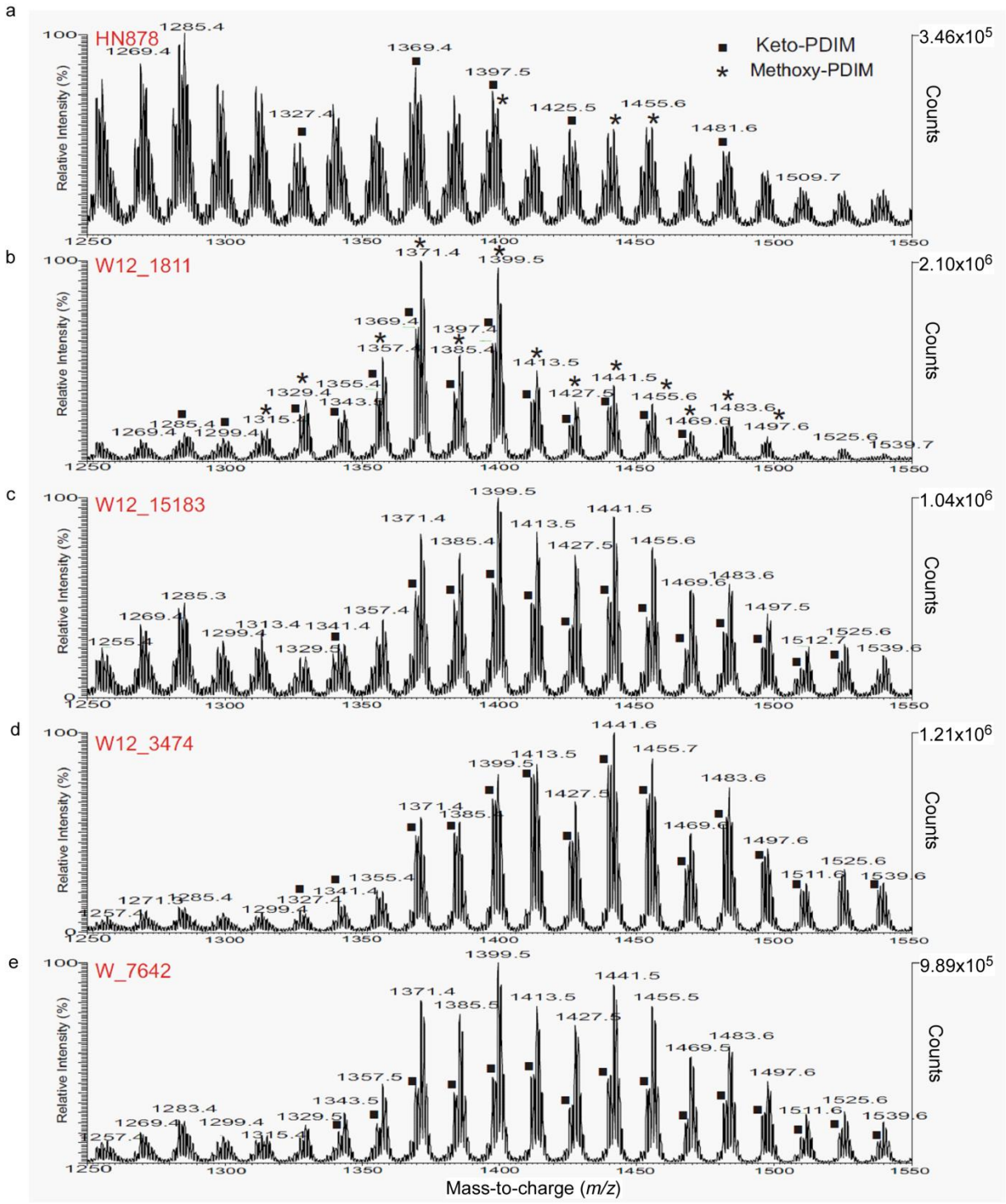


Howard et al., Supplementary Figure 12

**Supplementary Figure 12. PDIM overexpression in MDR W-*Mtb*.** PDIM spectra were generated from extracted total lipid from *Mtb* strains HN878 (a), W12_1811 (b), W12_15183 (c), W12_3474 (d) and W_7642 (e). Spectra show relative abundance, normalized to the most abundant ions in each sample (left y-axis). Absolute count values for the most abundant ions are also shown (right y-axis). Trace data of HN878 and W_7642 is representative of at least two replicates; trace data of W12_1811, W12_15183, and W12_3474 represent a single run.

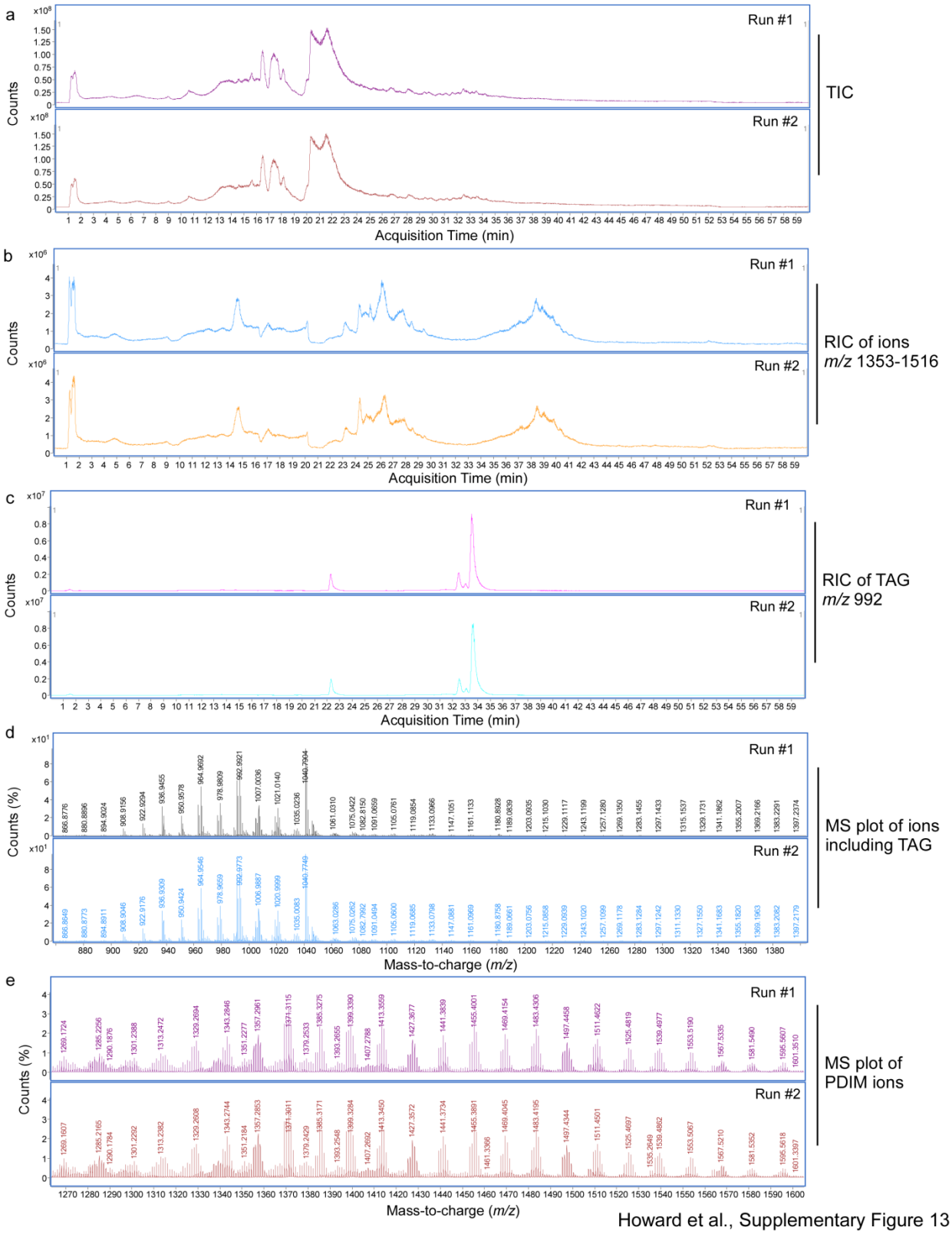


Howard et al., Supplementary Figure 13

**Supplementary Figure 13. PDIM expression by LC/MS is highly reproducible.** HN878 lipid extracts were independently analyzed twice. TIC plots (a), RIC plots of ions of *m/z* 1353-1516 (b), RIC plots of TAG internal standard at *m/z* 992 (c), MS plot of ions eluted from 31.43-34.48 min including TAG internal standard at *m/z* 992 (d), and MS plot of ions eluted from 36.68-41.16 min representing PDIM ions (e) are shown for the two runs.

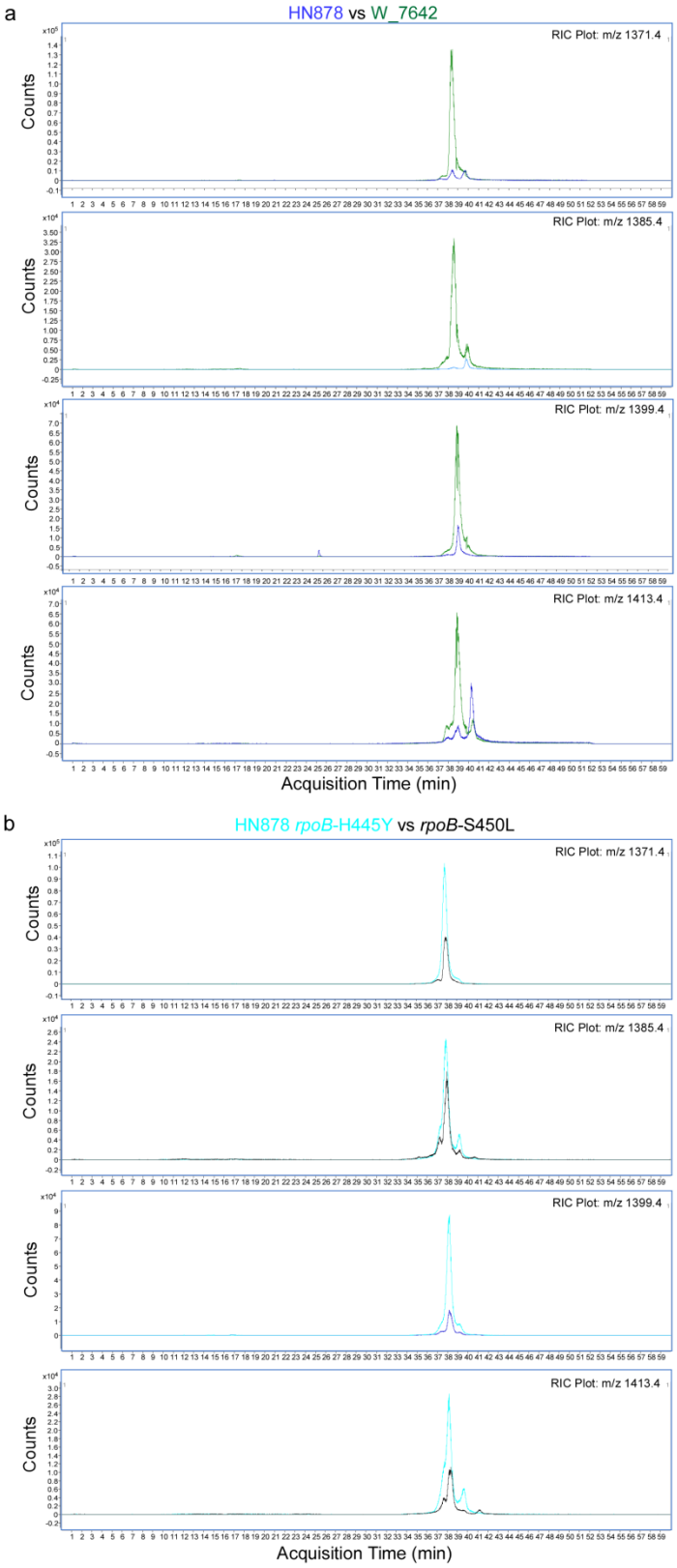


Howard et al., Supplementary Figure 14

**Supplementary Figure 14. Comparison of individual PDIM ions expressed by *Mtb* strains.** RIC plots for PDIM ions at *m/z* 1371.4, 1385.4, 1399.4, and 1413.4, comparing HN878 and W_7642, or HN878 *rpoB*-H455Y and *rpoB*-S450L. The blue trace represents HN878, and the green trace represents W_7642 (a). The blue trace represents HN878 *rpoB*-H445Y, and the black trace represents HN878 *rpoB*-S450L (b).

**SNPS potentially contributing to dispensability of IL-1R1**

| Position | Strand | Effect | Gene | Gene ID | Product | HGVS_C | HGVS_P | AL 123456 | HN878 | W12_1811 | W12_15183 | W12_3474 | W_7642 |
|---|---|---|---|---|---|---|---|---|---|---|---|---|---|
| 761139 | + | missense_variant | rpoB | Rv0667 | DNA-directed RNA polymerase (beta chain) RpoB (transcriptase beta chain) (RNA polymerase beta | c.1333C>T | p.His445Tyr | C | C | C | T | T | T |
| 1817295 | + | synonymous_variant | pykA | Rv1617 | Probable pyruvate kinase PykA | c.1107C>T | p.Ala369Ala | C | C | C | T | T | T |

**SNPS shared by W_7642 and W12_15183, but not W12_3474**

| Position | Strand | Effect | Gene | Gene ID | Product | HGVS_C | HGVS_P | AL 123456 | HN878 | W12_1811 | W12_15183 | W12_3474 | W_7642 |
|---|---|---|---|---|---|---|---|---|---|---|---|---|---|
| 761494 | + | missense_variant | rpoB | Rv0667 | DNA-directed RNA polymerase (beta chain) RpoB (transcriptase beta chain) (RNA polymerase beta subunit) | c.1688A>C | p.Glu563Ala | A | A | A | C | A | C |
| 800914 | + | missense_variant | rplC | Rv0701 | 50S ribosomal protein L3 RplC | c.106G>T | p.Val36Leu | G | G | G | T | G | T |
| 1883151 | + | missense_variant | pks8 | Rv1662 | Probable polyketide synthase Pks8 | c.1448A>C | p.Glu483Ala | A | A | A | C | A | C |
| 2289103 | - | missense_variant | pncA | Rv2043c | Pyrazinamidase/nicotinamidase PncA (PZase) | c.139A>G | p.Thr47Ala | T | T | T | C | T | C |
| 3064841 | - | missense_variant | Rv2752c | Rv2752c | Conserved hypothetical protein | c.1351G>A | p.Gly451Ser | C | C | C | T | C | T |
| 3408968 | - | synonymous_variant | nrdF2 | Rv3048c | Ribonucleoside-diphosphate reductase (beta chain) | c.411G>A | p.Gln137Gln | C | C | C | T | C | T |

**SNPS unique to W_7642**

| Position | Strand | Effect | Gene | Gene ID | Product | HGVS_C | HGVS_P | AL 123456 | HN878 | W12_1811 | W12_15183 | W12_3474 | W_7642 |
|---|---|---|---|---|---|---|---|---|---|---|---|---|---|
| 55553 | + | missense_variant | ponA1 | Rv0050 | Probable bifunctional penicillin-binding protein 1A/1B PonA1 (murein polymerase) (PBP1): penicillin-insensitive transglycosylase (peptidoglycan TGASE) penicillin-sensitive transpeptidase (DD-transpeptidase) | c.1891C>T | p.Pro631Ser | C | C | C | C | C | T |
| 827513 | | | | | intergenic region | | | G | G | G | G | G | T |
| 2337253 | + | missense_variant | Rv2079 | Rv2079 | Conserved hypothetical protein | c.1899T>G | p.Ile633Met | T | T | T | T | T | G |
| 3589116 | + | missense_variant | rhlE | Rv3211 | Probable ATP-dependent RNA helicase RhlE | c.1319C>G | p.Thr440Arg | C | C | C | C | C | G |

**SNPS shared by W_7642 and reference strain H37Rv or HN878**

| Position | Strand | Effect | Gene | Gene ID | Product | HGVS_C | HGVS_P | AL 123456 | HN878 | W12_1811 | W12_15183 | W12_3474 | W_7642 |
|---|---|---|---|---|---|---|---|---|---|---|---|---|---|
| 206481 | + | synonymous_variant | mce1F | Rv0174 | Mce-family protein Mce1F | c.1251C>G | p.Pro417Pro | C | G | G | G | G | C |
| 278021 | + | synonymous_variant | Rv0232 | Rv0232 | Probable transcriptional regulatory protein (probably TetR/AcrR-family) | c.123T>C | p.Arg41Arg | T | C | C | C | C | T |
| 302797 | | | | | intergenic region | | | T | T | C | T | T | T |
| 761155 | + | missense_variant | rpoB | Rv0667 | DNA-directed RNA polymerase (beta chain) RpoB (transcriptase beta chain) (RNA polymerase beta subunit) | c.1349C>T | p.Ser450Leu | C | C | T | C | C | C |
| 826717 | + | synonymous_variant | mapA | Rv0734 | Methionine aminopeptidase MapA (map) (peptidase M) (MetAP) | c.48C>T | p.Arg16Arg | C | C | T | T | T | C |
| 1079927 | + | synonymous_variant | ctpV | Rv0969 | Probable metal cation transporter P-type ATPase CtpV | c.1185C>A | p.Thr395Thr | C | A | A | A | A | C |
| 1080192 | + | missense_variant | ctpV | Rv0969 | Probable metal cation transporter P-type ATPase CtpV | c.1450G>A | p.Asp484Asn | G | A | A | A | A | G |
| 2235087 | - | synonymous_variant | ctpG | Rv1992c | Probable metal cation transporter P-type ATPase G CtpG | c.2220C>T | p.Phe740Phe | G | A | A | A | A | G |
| 2289016 | - | missense_variant | pncA | Rv2043c | Pyrazinamidase/nicotinamidase PncA (PZase) | c.226A>C | p.Thr76Pro | T | T | G | T | T | T |
| 2533377 | + | synonymous_variant | Rv2260 | Rv2260 | Conserved hypothetical protein | c.48T>C | p.Asp16Asp | T | C | T | C | C | C |
| 3034607 | - | synonymous_variant | Rv2721c | Rv2721c | Possible conserved transmembrane alanine and glycine rich protein | c.13A>C | p.Arg5Arg | T | T | G | T | T | T |
| 3690947 | | | | | intergenic region | | | A | A | G | A | A | A |

Howard et al., Supplementary Table 1

**Supplementary Table 1. Identification of unique SNPs that mediate macrophage reprogramming in W-MDR** *Mtb*. Based on WGS of *Mtb* strains, all SNPs that distinguished between W12_1811 and W_7642 were determined (24 SNPs). From there, we eliminated all SNPs shared between W_7642 and the reference strain, H37Rv, or HN878 (highlighted blue, 12 SNPs), as well as SNPs unique to W_7642 (highlighted green, 4 SNPs) or shared by only W_7642 and W12_15183, but not W12_3474 (highlighted red, 6 SNPs). This identified two SNPs shared by W_7642, W12_15183, and W12_3474 (highlighted yellow, 2 SNPs) namely *rpoB*-H445Y and *pykA*-A369A as potential mediators of macrophage reprogramming.